Comparisons betweenV_{S30} and Spectral Response for 30 sites in Newcastle, Australia from collocated Seismic Cone Penetrometer, Active- and Passive-Source V_S Data

T. Volti, C. Collins, C. H. Pascal & J. Holzschuh

Geoscience Australia, GPO Box 378, Canberra ACT 2601, Australia.

D. Burbidge

GNS Science, Avalon, Lower Hutt, NZ.

M. Asten

School of Geosciences, Monash University Melbourne.

J. Odum & W. Stephenson

Geologic Hazards Science Center, U. S. Geological Survey.

ABSTRACT: We make extensive use of different methodologies in order to question the applicability of amplification factors (AF) as defined by V_{S30}, for 30 sites in the Newcastle area, Australia. This includes seismic cone penetrometer (SCP) and spectral analysis of surface waves (SASW), horizontal-to-vertical spectral ratio (H/V), surface-wave spatial autocorrelation (SPAC), refraction microtremor (ReMi) and multichannel analysis of surface waves (MASW) data. We show that V_{S30} is related to spectral response but not necessarily with the maximum amplification. Transition zones within the geological units may be important factors influencing site effects. Both V_{S30} and AF values are influenced by the velocity ratio between bedrock and overlying sediments and the presence of surficial thin low velocity layers (STL) (< 2m thick and < 150 m/s), but the velocity ratio is what affects mostly the AF. At $0.2 < T < 0.4$ s, the AFs are largely influenced by surficial geology. For $T > 0.5$ s, amplification curves follow the order expected for hard to soft site classes. The SPAC and ReMi techniques have the smallest deviation from the average AF for all sites, corresponding to a factor of < 0.5 for > 75% of the data.

1 INTRODUCTION

Several methods exist for calculating V_{S30}, each with its own advantages and limitations. For this reason, multi-method approaches have been used in the recent past (Odum et al., 2013; Stephenson et al., 2015) to compare different techniques and add confidence to the characterization information that has been obtained from the analysis of shear wave velocity profiles (SWVP) for site effects. However, to the best of our knowledge, explored comparisons between V_{S30} estimation approaches use a limited number of techniques. In this paper, for the first time, we make extensive use of different methodologies as blind comparisons.

Controversy exists about the limitations of V_{s30} when used as a single parameter for the prediction of amplification and in complex geological settings. Possible resolution and suggestions on this controversy are very important for public safety, as V_{S30} is extensively used by the earthquake engineering

community. In order to address the above problems a dataset of V_{S30} measurements was gathered and assessed for the Newcastle area, NSW, Australia. The 1989 Newcastle earthquake, while registering a M_L 5.6, killed thirteen people and caused extensive damage to residential and commercial buildings, particularly unreinforced masonry structures.

Depending on the type of wave source used, V_{S30} can be measured by active methods, such as spectral analysis of surface waves, (SASW) (Nazarian et al., 1983), and multichannel analysis of surface waves (MASW) (Park et al., 1999) and body-wave reflection/refraction (Williams et al., 2005) or passive methods such as reflection microtremor (ReMi) (Louie, 2001), passive MASW (Park et al., 2007) and spatial autocorrelation, (SPAC) (Aki, 1957; Horike, 1985, Asten, 2006) and the horizontal-to-vertical spectral ratio method (H/V) (Nakamura, 1989). What all the above techniques have in common is that they are non-invasive, inexpensive and use portable equipment, in contrast to boreholes or seismic cone penetrometer (SCP) which are environmentally invasive, expensive and have limited applicability to stiff or rock sites.

2 FIELDWORK

During 2012 and 2013, Geoscience Australia (GA) collaborated with Monash University (MU) and U.S Geological Survey (USGS) to study near-surface shear-wave velocities in and around the city of Newcastle. In March 2012, GA and MU jointly deployed micro-arrays for the acquisition of microtremor data for processing using the spatial autocorrelation (SPAC) method. These data were also processed using the multi-mode SPAC (MMSPAC) method (Asten, 2013), in which the vertical component microtremor wave-field is forward modelled by direct curve fitting in the spectral coherency domain, with observed H/V used qualitatively to assess goodness of fit with the model theoretical Rayleigh ellipticity. Henceforth, to distinguish between models from the two SPAC processing approaches, they will be referred as SPAC1 (using NA) and SPAC2 (MMSPAC), respectively.

In April 2013, MASW, P- and S-wave refraction and another set of microtremor data were acquired by GA. Active and passive data were processed by GA using the SeisImager (SeisImager/SW™ Manual, 2009) while the passive data were further processed by USGS using the SeisOpt®-ReMi™ software. (Odum et al., 2013), with abbreviations M+PM (GA) and ReMi (USGS), respectively. Data from a total of 30 sites were collected during the two consecutive field campaigns. Past acquired spectral analysis of surface waves (SASW) data (Collins et al., 2006; Kayen et al., 2014) are also shown (Fig. 1). The selection of sites was based on near-surface materials associated with the regional geology (McPherson and Hall, 2013) and previous SCP data (Dhu and Jones, 2002; Crump, 2001).

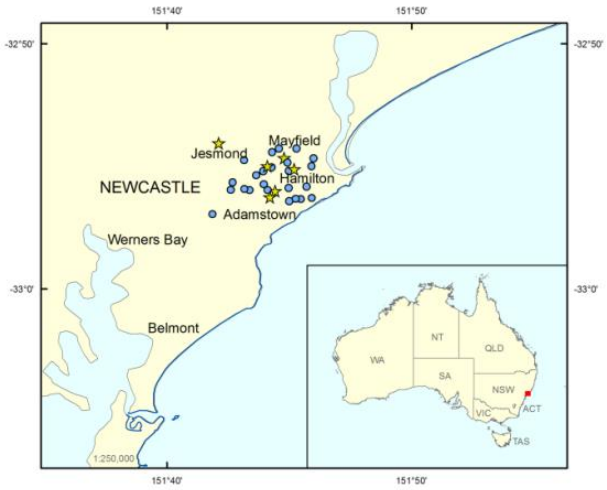

Figure 1. Map of Newcastle area. Blue and yellow dots are site locations where new data was acquired during this study. Yellow stars denote sites where previous data was acquired using the SASW method. Inlet shows the location of the survey area (red square) in Australia.

The acquisition of SCPs in the Newcastle area is described in Crump, (2001). A bedrock V_S value of 1700 m/s was assumed in all cases. Additional data from six sites (yellow stars) are from a collaborative project with the USGS that used the SASW method. The results from the SCP and SASW data acquisition projects were included in the comparative analysis presented in this paper.

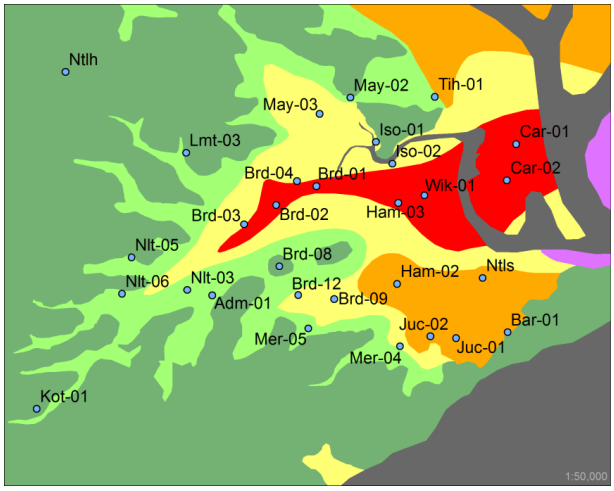

Figure 2. Site locations with respect to local geological conditions. Green: weathered rock. Light green: Silt and clay. Yellow: Sand overlying silt and clay. Orange: Silt and clay with interbedded sand. Red: Sand with interbedded silt and clay. Purple: Barrier island sand. Bedrock is of Permian-Triassic age.

3 V_{S30} RESULTS

V_{S30} values and depth to bedrock for all methods are shown in Figure 3. The five site classes in Figure 2 are grouped into five blocks equally distributed along the x-axis and separated by dashed lines. The names of classes correspond to the colour map of the same figure.

Class 1 (left side of Fig.3a) represents relatively hard rock, whereas Class 5 (right) contains sites located on relatively softer soil. V_{S30} values decrease from ~700 m/s to ~200 m/s, corresponding to classes C-D from the NEHRP building code classification (Kayen et al., 2013). Bedrock depths increase from ~5 m to a maximum of 50 m from left to right (Fig.3b).

Generally, M+PM and ReMi V_{s30} values fall in between their corresponding SPAC results. The biggest scatter in V_{S30} values is observed in Class 1. Bedrock depth for Class 1 is similar to Class 2. For Class 1, two reasons may be responsible for the scatter in V_{S30} values: the presence or absence of a surficial thin (<2m) low velocity layer (<150 m/s) (STL) for the majority of sites in Class 1, and the high bedrock velocity, both effects observed for the SPAC methods. The former can significantly lower the value of V_{S30}, while the latter increase it.

Class 5, which is the softest and probably the most important from the point of view of seismic hazard, shows the best agreement between methods in V_{S30} value. Note that the average depth to bedrock, regardless of method, decreases significantly for all other sites, which are located westwards and subsequently covered by thinner layers of sediments.

Bedrock depth estimates increase with the progressively softer site classes. For the majority of sites, the M+PM method resulted in profiles with smaller velocity contrasts compared with the other methods and therefore V_{S30} values remained low (Fig.3a).

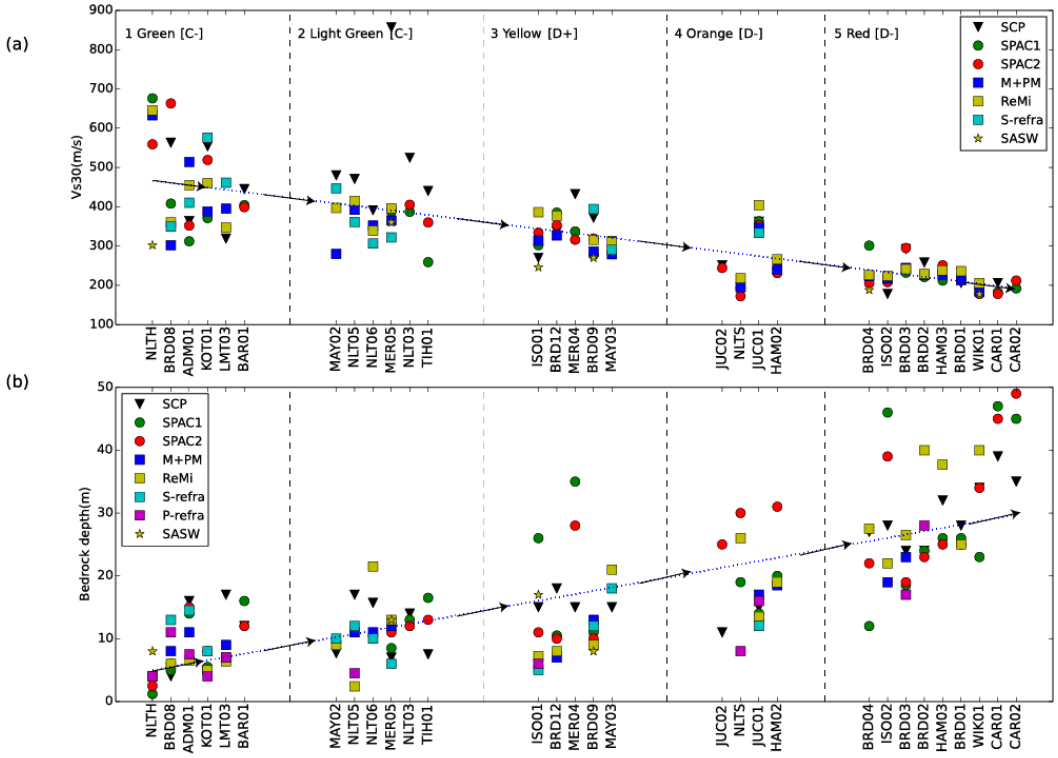

Figure 3. For all methods used (a) V_{S30} vs site class (b) Bedrock depth vs site class. Site classes as seen in Fig.2: 1- Green: Weathered rock. 2- Light Green: Silt and clay over weathered rock. 3- Yellow: Thin sand over silt and clay. 4- Orange: Silt and clay with interbedded sand. 5- Red: Sand with interbedded silt and clay. Letters in square brackets denote the corresponding site class in the NEHRC system. A regression line is fitted to the data (dotted blue line). Black lines emphasize the direction of change.

STLs were modelled for sites ADM01, BRD03, BRD04, BRD08, BRD12, HAM02, HAM03, ISO02, KOT01 and TIH01 using SPAC1. The resulting V_{S30} values were significantly smaller especially when compared with SPAC2 except BRD12, where a STL was a common feature for both methods. For several sites SCP showed comparable surficial layers with those from SPAC1.

P-wave refraction travel-time models showed poor agreement with the other methods, including S-wave refraction. This was because the majority of profiles showed a fast layer present at < 5 m depth. This shallow layer was believed to be the water table, and these sites were subsequently omitted. When a third layer could be discerned in the records, the results were included in Figure 3.

For the depth to bedrock, the S-wave refraction results are below average for the softer sites. For Class 5, S-refraction couldn't discern the deep bedrock at all, as no refracted arrivals were recorded at far offsets. S-wave refraction will not show the water table as S-waves only travel through solids.

Several sites are geographically located close to the edge of a certain lithological class (represented by colour), some well toward the centre, yet others are located near the edge of two or more different classes (Fig.2). We tried to arrange the site sequence within each class according to their relative position to the bordering class, and select one out of the two (or more) different classes for the sites located on bordering lines. Using both geological information and V_{S30} results can be useful in the construction of site zonation maps.

4 SITE AMPLIFICATION

In this section, we use the SUA (Seismic hazard Uncertainty Analysis) package (Robinson et al., 2006), to illustrate the effect on the regolith site response derived from the different techniques. This is based on the equivalent linear approach (Bardet et al., 2000; Idriss and Sun, 1992). The 2012/08/06 Tamworth earthquake, M_L4.2, 280 km from Newcastle, was used as input rock motion for the modelling process. Modulus reduction and damping ratio curves were taken from average values of rock, clay and sand.

We calculate the amplification factors AF and the resonant periods RP (where the max amplification factor is observed) from the observed velocity profiles. In Fig.4a, the AFs oscillate between 1.4 and 3.9 among the different methods (giving a difference of a factor of 3), with no trend related to site classes (the smaller scatter is observed for Class 5. The regolith V_S varies significantly with different sites, and we only occasionally observe low velocity layers, and these are generally thin (i.e. STL). Class 1 is not pure rock but weathered rock, with several meters of silty clay.

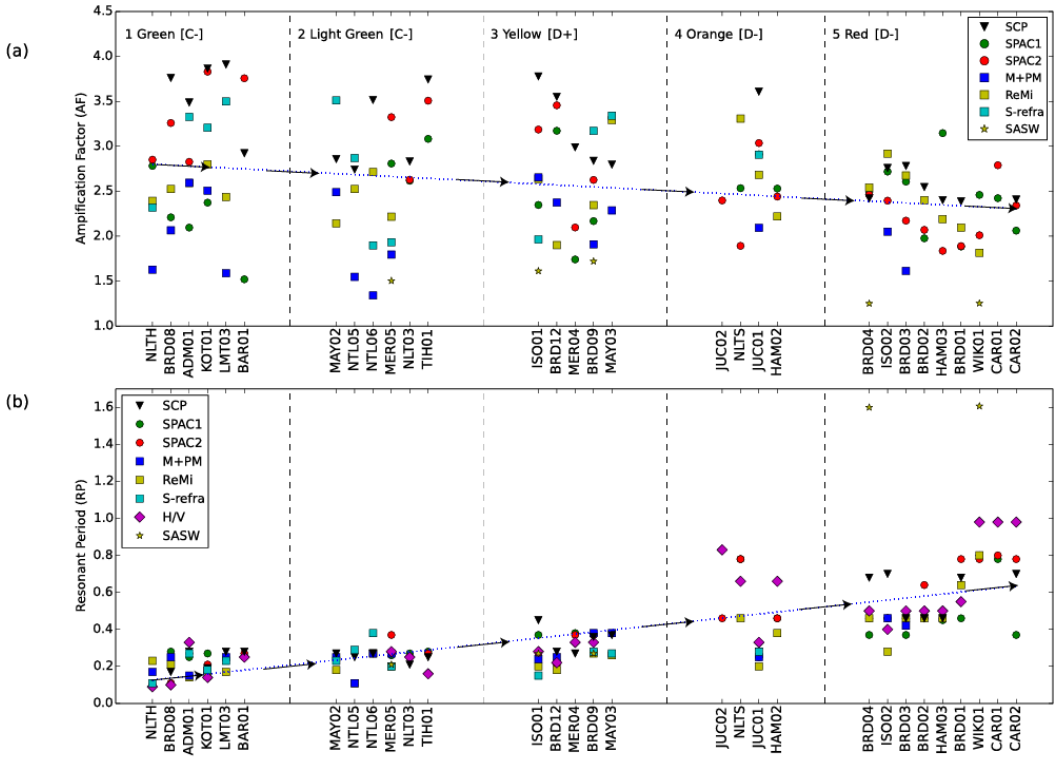

Figure 4. For most methods used (a) Amplification factors (AF) vs site class and (b) Resonant Periods (RP) vs site class. Site classes: 1- Green: Weathered rock. 2- Light green: Silt and clay over weathered rock. 3- Yellow: Thin sand over silt and clay. 4- Orange: Silt and clay with interbedded sand. 5- Red: Sand with interbedded silt and clay. Letters in square brackets denote the corresponding site classes in the NEHRC system. A regression line is fitted to the data (dotted blue line). Black arrows emphasize the direction of change.

Higher AF values are observed for those sites and methods where there is high velocity ratio (SPAC2 and S-wave refraction). High AFs can be related to shallow bedrocks, as energy tends to accumulate near surface, especially if there is a large velocity ratio. This could be the reason why Class 1 has the highest AFs overall observed. High AFs also occur at shorter periods (Fig.5). Bar01 for SPAC2 (max AF 3.7) has one of the highest velocity ratios and although V_{S30} is similar to SPAC1, their AFs difference is due to different velocity ratios from the two methods. This is also confirmed by our modelling, where AFs ~ 3.2 are calculated for $V_{S\_bedrock}$ /$V_{S\_regolith}$ > 3.5 and bedrock depths of < 25 m. There may be another factor affecting the AF, as the modelling indicates. When the regolith V_S is low and the

bedrock depth shallow, AFs tend to be high at shorter periods even for smaller velocity ratios. Both our data and modelling indicate that high velocity ratio is the factor contributing the most.

There are some cases where shallow bedrock is related to low amplification. The low values for the M+PM method are mostly observed for Class 5, where the bedrock is deep, the regolith V_S low, and the method failed to 'see' the bedrock (gradational velocity models are responsible for low AFs).

The shape of the amplification curve (AC) can also reveal further information related to local maximums at other periods that may correlate with the natural period of buildings. For each class, the median value was calculated for the whole AC (Fig.5). SASW method was excluded as the very few results available had unusually low AFs. For period T > 0.5 s, the order of the ACs agree with the response spectra for hard to soft soil classes (Standard Australia, 2007), with Class 5 materials having a much higher amplification than the other types. The variations at T > 1 s are believed to be due to the characteristics of the input source earthquake. On the other hand, for T < 0.5 s, the AFs are most likely related to local surficial differences, including the class classifications. As we have seen before, shifting sites in and among classes plays a significant role in establishing a meaningful trend in V_{S30} values and the order of the maximum AFs for T < 0.5 s may be heavily influenced by the transition zones between the different geological formations. Standard deviation is very large at these low periods, while at longer periods it diminishes. For some classes (i.e. Class 3) it is much greater than the curves themselves, rendering the median values statistically insignificant. However, for 0.5 <T < 1.5 s, the scattering diminishes.

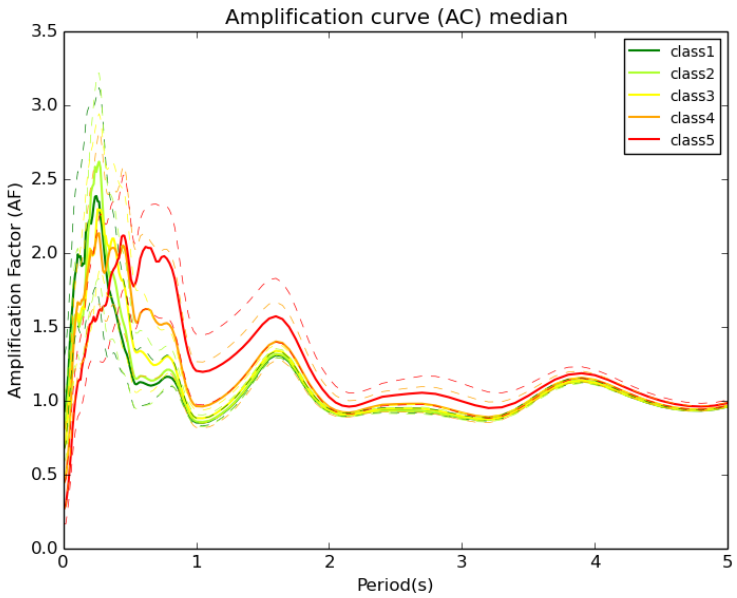

Figure 5 *Amplification curve (AC) median for all techniques and site classes. Site class: Green: Weathered rock. Light green: Silt and clay. Yellow: Thin sand over silt and clay. Orange: Silt and clay with interbedded sand. Red: Sand with interbedded silt and clay. Dashed lines denote +/-1 standard deviation for each class.*

5 **DISCUSSION**

Different types of measurements show variability in results at each site. Despite the differences, V_{S30}, bedrock depth and RP, examined across the five soil types of Figure 2, exhibit the following trends from firm soil (weathered rock) to soft soil (sand-silk-clay): V_{S30} decreases, while bedrock depth and RP increase. Slight reorganisation of the sites in relation to the regional geology, gives more meaningful trends in the above three parameters (compared with random intra- and inter-positioning), suggesting that the geological boundaries displayed on Figure 2 may need to be redrawn due to extended transition zones between classes.

Our results suggest that although V_{S30} estimations do correspond to the NEHRP or AS1170.4 building codes, there is no overall correlation between V_{s30} and amplification (Castellaro et al., 2008; Zaslavsky et al., 2012). The maximum AFs, being observed at short periods ($0.2<T<0.4$ s) are scattered and with large deviation, largely influenced by surficial geology and complications arising between the different geological formations. However, for $T > 0.5$ s, the AC for all classes follow the order expected when transition exists from hard to soft site classes.

Our results have shown agreement for the regolith velocity but large variation for the bedrock velocity. Given the fact that the velocity contrast between bedrock and the overlying regolith is crucial for the AF, this may be the most important limitation in amplification studies using V_{S30} techniques, where the bedrock velocity remains an assumption even in the case of the SCP.

STLs can lower V_{s30} and increase AF values. Not all methods can detect the presence of STLs. If SCP is the most realistic method (though obtrusive) SPAC1 (and to a lesser degree SPAC2 and ReMi) is the only method that captures the surficial changes seen in SCP. As the variation between models has shown, even a little change in the input model can significantly affect the AF. A model that captures more details of the subsurface under a site is therefore much more valuable than a simplified one.

In general, where the difference between methods is more than ~20%, the variation can be attributed to inherent method limitations and/or acquisition parameters. SPAC1, SPAC2 and ReMi methods, due to their lower frequency content, provided better imaging over depth, capturing the bedrock where it was deep. In contrast, P- and S-wave refraction showed limitations due to poor-signal to noise ratio for far offsets required for deeper bedrock refractions. Improvement in far offset first arrivals in the refraction data could provide bedrock velocities and depth. M+PM and ReMi data interpretation by two independent groups resulted in bedrock Vs discrepancies, while M+PM showed inability to 'see' the bedrock especially at sites with low Vs due to unconsolidated sediments.

The AF values can nevertheless be used for a relative comparison between the different techniques. For that, the median and standard deviation at each site are calculated, and grouped together for each technique. Figure 6 shows the deviation from the median for all techniques. For the arbitrary amplification factor of 0.5 (which corresponds to a difference of half a given median amplification value), 60% (SCP), 75% (SPAC1 and SPAC2) and 87% (ReMi) lay below 0.5. These are the smallest deviations for all techniques. Assuming that the median trend is a 'true' representation of the AF, half a factor in amplification uncertainty is still acceptable for seismic hazard and so, from this point of view passive methods seem to be more appropriate. From the point of view of seismic engineering, overestimation of AF for a particular area would lead to fewer casualties than underestimation. In this sense, SCP and SPAC2 methods give best results.

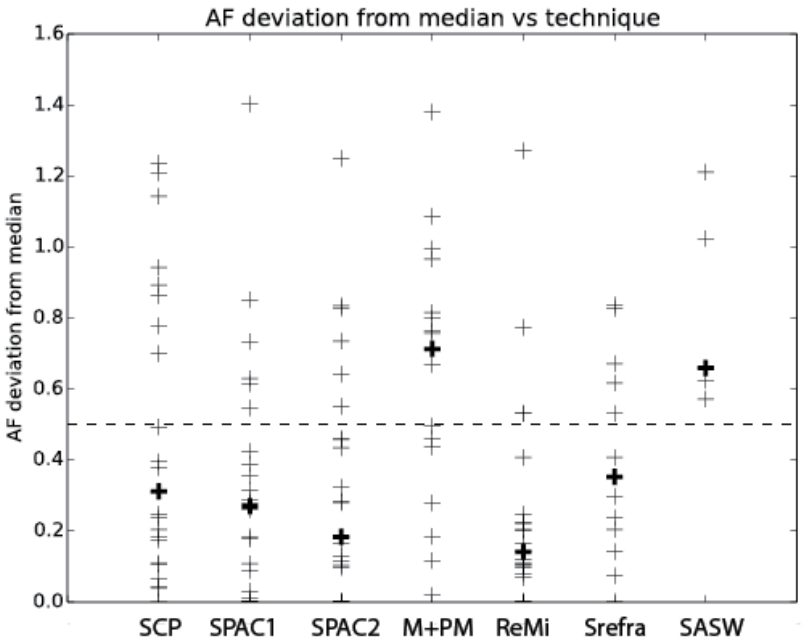

Figure 6 Amplification factor (AF) deviation from the median for each site. The different techniques are then separately grouped. The crosses show measurements for all techniques. Dark crosses represent the median (from the deviation from median) for each technique. Dashed line is an arbitrary cut-off of 0.5 for the AF deviation.

6 **CONCLUSIONS**

1. $V_{S30,}$ depth to bedrock and resonant period are well correlated with the regional geology, but not the maximum amplification (AF). Instead of the AF, the spectral response at T > 0.5 s increases for hard to soft site classes.
2. Consideration of site location in relation to the regional geology gives more meaningful V_{S30} and bedrock depth values than random arrangement within clusters. Slight rearrangement of sites located at edges of different formations suggests that the geological boundaries may need to be redrawn due to transition zones.
3. A large velocity ratio between regolith and bedrock is the most important parameter affecting the AF. The velocity of the bedrock has shown large discrepancy among techniques, and therefore is the source of the most uncertainty in calculating the AF.
4. Comparison between the different techniques shows that:
    a. Surficial thin low velocity layers are important for V_{s30} estimation and the amplification. Methods such as SPAC1 and SCP are more capable to detect these layers.
    b. From a hazard point of view, SPAC2, SCP and S-wave refraction profiles, resulting in high velocity ratios and consequently higher AF values, are preferable over M+PM and SASW (low velocity ratios).
    c. Passive methods (SPAC1, SPAC2 and ReMi) give the smallest deviations from the AF median and therefore are preferable over active methods. The SPAC1 and SPAC2 techniques have smaller discrepancies in bedrock V_S than M+PM and ReMi techniques, and therefore are the most reliable among the passive methods.
5. V_{S30} estimation is a highly empirical process. Further method refinement may be needed to understand and/or reduce the observed difference among techniques. Given that each technique has its own advantages as well as limitations, a careful examination and comparison can potentially bring forth fruitful results.

REFERENCES:

Aki, K., 1957. Space and time spectra of stationary stochastic waves, with special reference to microtremors. *Bulletin of the Earthquake Research Institute*, 35, 415-457.

Asten, M.W., 2006. On bias and noise in passive seismic data from finite circular array data processed using SPAC methods: *Geophysics*, 71 (6), V153-V162.

Asten, M.W., Collins, C., Volti, T. and T. Ikeda, 2013. The good, the bad and the ugly – lessons from and methodologies for extracting shear-wave velocity profiles from microtremor array measurements in urban Newcastle, NSW: *Extended Abstracts of the 23rd ASEG Conference and Exhibition,* http://www.publish.csiro.au/nid/267.htm

Borcherdt, R.D., 1994. Estimates of site-dependent response spectra for design (methodology and justification). *Earthquake Spectra* 10, 617-653.

Building Seismic Safety Council, 2004. NEHRP Recommended Provisions for seismic regulations for new buildings and other structures (FEMA 450). Building Seismic Safety Council, National Institute of Building Sciences. Washington D.C.

Castellaro, S., Mulargia, F. and P.L. Rossi, 2008. V_{s30}: Proxy for seismic amplification? *Seismol. Res. Lett.* 79, 540–543.

Collins, C., Kayen, R., Carkin, B., Allen, T., Cummins, P. & McPherson, A. 2006. Shear wave velocity measurement at Australian ground motion seismometer sites by the spectral analysis of surface waves (SASW) method. *Earthquake Engineering in Australia, Canberra, ACT, November 24-26, 2006, Proceedings: Australian Earthquake Engineering Society*, 173-178.

Crump, C., 2001. Seismic amplification of alluvial soils in the Newcastle Basin. (IVL 4550). Dept. of Civil, surveying and environmental engineering, The University of Newcastle, Australia.

Dhu, T. and T. Jones (editors), 2002. Earthquake Risk in Newcastle and Lake Macquarie. *Rec. Geosci. Aust.* Record 2002/15, Geoscience Australia, Canberra.

Kayen, R.E., Carkin, B.A., Allen, T., Collins, C., McPherson, A. & Minasian, D. 2014. *Shear-wave velocity and site-amplification factors for 50 Australian sites determined by the spectral analysis of surface waves method*. U.S. Geological Survey, Open-File Report 2014–1264, 118 pp, http:/dx.doi.org/10.3133/ofr20141264.

Louie, J.N., 2001. Faster, better shear-wave velocity to 100meters depth from refraction microtremor arrays, *Bull. Seismol. Soc. Am.* 91, 347–364.

McNamara, D.E., Stephenson, W.J., Odum, J.K., Williams, R.A. and L. Gee (2014). Site response in the eastern United States: A comparison of Vs30 measurements with estimates from horizontal:vertical spectral ratios, *Geological Society of America Special Papers*,509, p. SPE 509-04, first published on September 30, 2014, doi:10.1130/2015.2509(04).

McPherson, A. and L. Hall, 2013. Site Classification for Earthquake Hazard and Risk Assessment in Australia. *Bulletin of the Seismological Society of America* April 2013 103:1085-1102.

McPherson, A. and L. Hall, 2007. Development of the Australian National Regolith Site Classification Map, *Rec. Geosci. Aust.* 2007, no. 7, Australian Government, Canberra. 37. Available at:https://www.ga.gov.au/products/servlet/controller?event=GEOCAT_DETAILS &catno=65240

Nakamura, Y., 1989. A method for dynamic characteristics estimation of subsurface using microtremor on the ground surface: *Quality report* of RTRI. Railway Technical Research Institute/Tetsudo Gijutsu Kenkyujo, Japan, 25-33.

Nazarian, S.K., Stokoe K. and W. Hudson, 1983. Use of spectral analysis of surface waves method for determination of moduli and thicknesses of pavement systems *Transportation Research Record* no. 930, 38-45.

NSW Department of Public Works and Services, 1998. Clarence/Coffs Harbour Regional Water Supply – Shannon Creek Dam Site, Concept Design Stage, *Geological Investigation*, 97, GC58A 1.

Odum, J.K., Stephenson, W.J., Williams, R.A. and C. von Hillebrandt-Andrade, 2013. V_{s30} and spectral response from collocated shallow, active- and passive-source Vs data at 27 sites in Puerto Rico, *Bulletin Seismological Society of America*, v. 103, no. 5, p. 2709-2728, doi:10.1785/0120120311.

Park, C.B., Miller, R.D., and J. Xia, 1999. Multichannel analysis of surface waves (MASW). *Geophysics*, 64, 800-808.

Robinson, D., Dhu, T. and J. Schneider, 2006. SUA: A computer program to compute regolith site-response and estimate uncertainty for probabilistic seismic hazard analyses, *Comput. Geosci.* 32, 109–123.

Standards Australia, 2007. Minimum design loads on structures (known as the SSA Loading Code), AS1170.4-2007 Part 4: Earthquake loads (2nd edition). *Standards Australia* (Standards Association of Australia), Homebush, NSW.

Stephenson, W.J., Odum, J.K., McNamara, D.E., Williams, R.A. and S.J. Angster, 2015. Ground motion site effects from multi-method shear-wave velocity characterization at 16 seismograph stations deployed for aftershocks of the August 2011 Mineral, Virginia, earthquake, in J.W. Horton, M.C. Chapman, and R.A. Green eds., *Geological Society of America Special* Paper 509: The 2011 Mineral, Virginia, Earthquake, and Its Significance for Seismic Hazards in Eastern North America, doi:10.1130/2015.2509(03).

Wathelet, M., Jongmans, D. and M. Ohrnberger, 2004. Surface wave inversion using a direct search algorithm

and its application to ambient vibration measurements. *Near Surface Geophysics*, 2:211–221.
Volti, T., Collins, C., Asten, M. and D. Burbidge, 2014. The 2012 Newcastle-Sydney SPAC microtremor surveys. Rec. *Geosci. Aust.* 2014/054. Geoscience Australia, Canberra. http://dx.doi.org/10.11636/Record.2014.054.
Zaslavsky, Y., Shapira, A., Gorstein, M., Perelman, N., Ataev, G. and T. Aksinenko, 2012. Questioning the applicability of soil amplification factors as defined by NEHRP (USA) and the Israel building standards. *Natural Science* 4, 631-639.